Inorg. Chem. **2003**, *42*, 4873–4880

Theoretical Characterization of Stable η^1-N_2O-, η^2-N_2O-, η^1-N_2-, and η^2-N_2-Bound Species: Intermediates in the Addition Reactions of Nitrogen Hydrides with the Pentacyanonitrosylferrate(II) Ion

José A. Olabe[†] and Guillermina L. Estiú*[,‡]

Departamento de Química Inorgánica, Analítica y Química Física, Inquimae, Facultad de Ciencias Exactas y Naturales, Universidad de Buenos Aires, Pabellón 2, Ciudad Universitaria, Buenos Aires C1428EHA, Argentina, and Departamento de Química, Cequinor, Facultad de Ciencias Exactas, Universidad Nacional de La Plata, 47 esq 115, La Plata B1900AVV, Argentina

Received November 18, 2002

The addition of nitrogen hydrides (hydrazine, hydroxylamine, ammonia, azide) to the pentacyanonitrosylferrate(II) ion has been analyzed by means of density functional calculations, focusing on the identification of stable intermediates along the reaction paths. Initial reversible adduct formation and further decomposition lead to the η^1- and η^2-linkage isomers of N_2O and N_2, depending on the nucleophile. The intermediates (adducts and gas-releasing precursors) have been characterized at the B3LYP/6-31G** level of theory through the calculation of their structural and spectroscopic properties, modeling the solvent by means of a continuous approach. The η^2-N_2O isomer is formed at an initial stage of adduct decompositions with the hydrazine and azide adducts. Further conversion to the η^1-N_2O isomer is followed by Fe–N_2O dissociation. Only the η^1-N_2O isomer is predicted for the reaction with hydroxylamine, revealing a kinetically controlled N_2O formation. η^1-N_2 and η^2-N_2 isomers are also predicted as stable species.

Introduction

The electrophilic reactions of the nitrosyl ligand toward different nucleophiles (OH^-, nitrogen hydrides, thiolates, etc.) have been a subject of early concern.[1] Color tests using $[Fe(CN)_5NO]^{2-}$ (NP) to identify SH^- or SO_3^{2-} have been known for many years.[2] More recent reports refer to amines and thiols as reactive toward nitrosation, with the products being functionally described as possible NO^+ carriers in biological media.[3] Different $\{X_5MNO\}$ complexes have been used in reductive processes as electrophiles containing mainly group 8 metals, together with variable coligands (X) as ammonia, cyanides, and polypyridines, among others.[4,5] With the exception of OH^-, which leads to the corresponding nitro complexes,[6] other nucleophiles are irreversibly oxidized when the nitrosyl ligand is reduced. The stoichiometries of these processes are dependent on the nucleophile. Different nitrogen hydrides have been found to generate the following reaction patterns with NP:

$$[Fe(CN)_5NO]^{2-} + \begin{cases} N_2H_4 + OH^- \rightarrow [Fe(CN)_5H_2O]^{3-} + N_2O + NH_3 & (1)^7 \\ NH_2OH + OH^- \rightarrow [Fe(CN)_5H_2O]^{3-} + N_2O + H_2O & (2)^8 \\ NH_3 + OH^- \rightarrow [Fe(CN)_5H_2O]^{3-} + N_2 + H_2O & (3)^9 \\ N_3^- + H_2O \rightarrow [Fe(CN)_5H_2O]^{3-} + N_2 + N_2O & (4)^8 \end{cases}$$

All of these reactions are assumed to proceed through an initial reversible adduct formation between the N atoms of the nitrosyl ligand and the nucleophile. Although direct spectroscopic evidence affording a conclusive characterization of these adduct intermediates is generally lacking, recent studies performed with OH^-,[6] as well as with hydrazine (eq 1) and substituted derivatives,[7] allowed the elucidation of the geometries and spectroscopic properties of the stable adduct intermediates, based on density functional (DFT)

* To whom correspondence should be addressed. E-mail: estiu@biol.unlp.edu.ar.
† Universidad de Buenos Aires.
‡ Universidad Nacional de La Plata.

(1) Richter-Addo, G. B.; Legzdins, P. *Metal Nitrosyls*; Oxford University Press: New York, 1992.
(2) McCleverty, J. A. *Chem. Rev.* **1979**, *79*, 53−76.
(3) Stamler, J. S.; Singel, D. J.; Loscalzo, J. *Science* **1992**, *258*, 1898−1902.
(4) Bottomley, F. In *Reactions of Coordinated Ligands*; Braterman, P. S., Ed.; Plenum: New York, 1985; Vol. 2, pp 115−222.
(5) Lorkovic, I. M.; Ford, P. C. *Chem. Rev.* **2002**, *102*, 993−1018.
(6) Roncaroli, F.; Ruggiero, M. E.; Franco, D. W.; Estiú, G. L.; Olabe, J. A. *Inorg. Chem.* **2002**, *41*, 5760−5769.

10.1021/ic0261880 CCC: $25.00
Published on Web 07/16/2003

calculations. These adduct intermediates may either go back to the reactants or decompose intramolecularly by releasing gaseous products. The introduction of alkyl substituents at different positions of the hydrazine molecule was found to promote selectively the release of either N_2O, N_2, or mixtures of them.[7] This is also the case for the reactions 2−4 presented in this work. The stoichiometry and mechanism of these reactions depend on electron-counting factors associated with the structures of the nucleophiles, as well as on the kinetic routes that are available in each case. Overall, the detailed mechanisms of these adduct formations and decompositions are largely unknown.[4,5,10] Nevertheless, the accuracy attained in the above-mentioned calculations[6,7] prompted us to apply a similar theoretical approach to advance some mechanistic information for the other addition reactions.

In the above reactions, the anionic product $[Fe(CN)_5H_2O]^{3-}$ is able to coordinate the nitrite ion whenever it is present in the medium.[11] In favorable pH conditions (range 8−10), nitrite is transformed into bound NO (formally considered as NO^+).[6] Further attack of this species by an excess of nucleophile may lead to the onset of a catalytic process for nitrite reduction.[7] At this point, the reactions of the $[Fe(CN)_5H_2O]^{3-}$ ion appear as closely related to the behavior of some nitrite reductase enzymes,[12] which also react with nucleophiles in a similar way.[13] These enzymes, as well as others also related to denitrification processes occurring in natural systems, usually contain iron or copper in their reaction centers. The iron−porphyrin enzymes have a water-labile site capable of binding the nitrosyl ligand and of leading, then, to species with low-spin d^6 configurations. The structural mechanistic subtleties afforded by the different enzymes in order to release N_2, N_2O, or mixtures of them, are still open issues and matters of current interest.[12]

Given the well-known characterization of the pentacyano-L-ferrate(II) complexes for different L ligands,[14] and the accurate description afforded by DFT calculation for nitroprussiate and other related complexes,[6] we considered it worthy to extend the calculations on reaction 1 to reactions 2−4. For reaction 1, we have elucidated crucial mechanistic features, namely the structure of the adduct intermediate and the stabilization of linkage isomers of N_2O.[7] The coordination chemistry of N_2O with transition metals is still in its infancy.[10] Recent advances comprising the generation of linkage isomers of NO[15] and N_2[16] have shed light on the related behavior of other small molecules.[17] At this point, DFT calculations appear as a powerful tool to validate the characteristics of reaction intermediates and even propose the existence of others not experimentally captured at the present time. We present results that are valuable to predict and characterize possible N_2 or N_2O intermediates in the corresponding potential hypersurfaces for reactions 2−4.

Computational Methods

Calculations have been performed using Gaussian 98[18] and Becke's three-parameter hybrid functional[19] with LYP correlation functional (B3LYP).[20] Basis were of double-ζ split valence plus polarization quality (6-31G(d,p)). The structures have been fully optimized with no symmetry constrains. The true nature of the optimized minima has been verified, in each case, by means of the calculation of the harmonic frequencies. Time-dependent DFT (TD-DFT) calculations[21,22] were conducted to study the singlet excited states of the complexes. Transition states have been optimized, at the same level, following a quadratic synchronous transit algorithm. They were fully characterized by means of a vibrational analysis, leading to one imaginary frequency. A restricted approach was followed, on the basis of experimental EPR results, which indicated that no radical intermediates are formed in the course of the related addition reactions of hydrazine and substituted derivatives with nitroprusside.[7] Bulk solvent effects (water) are described via an isodensity continuum polarizable model.[23] The dielectric properties of the media have been found to influence the relative energies of the intermediates, as they involve species of different charges. Nevertheless, we are mainly interested in the structural characterization of the stable species that can be found along the reaction pathway, without attempting a more complex kinetic study, which should include a more thorough consideration of environmental and thermodynamic contributions. Moreover, the influence of the solvent has been recently considered in relevant theoretical studies on NO linkage isomers in nitroprusside, and a minor influence has been found in the calculated properties.[24]

(7) (a) Chevalier, A. A.; Gentil, L. A.; Amorebieta, V. T.; Gutiérrez, M. M.; Olabe, J. A. *J. Am. Chem. Soc.* **2000**, *122*, 11238−11239. (b) Gutiérrez, M. M.; Amorebieta, V. T.; Estiú, G. L.; Olabe, J. A. *J. Am. Chem. Soc.* **2002**, *124*, 10307−10319.

(8) Wolfe, S. K.; Andrade, C.; Swinehart, J. H. *Inorg. Chem.* **1974**, *13*, 2567−2572.

(9) (a) Katz, N. E.; Blesa, M. A.; Olabe, J. A.; Aymonino, P. J. *J. Inorg. Nucl. Chem.* **1980**, *42*, 581−585. (b) Maciejowska, I.; Stasicka, Z.; Stochel, G.; van Eldik, R. *J. Chem. Soc., Dalton Trans.* **1999**, 3643−3649. (c) Kenney, D. J.; Flynn, T. P.; Gallini, J. B. *J. Inorg. Nucl. Chem.* **1961**, *20*, 75.

(10) Trogler, W. C. *Coord. Chem. Rev.* **1999**, *187*, 303−327.

(11) Bradic, Z.; Pribanic, M.; Asperger, S. *J. Chem. Soc., Dalton Trans.* **1975**, 353−356.

(12) (a) Averill, B. A. *Chem. Rev.* **1996**, *96*, 2951−2964. (b) Hollocher, T. C. In *Nitric Oxide Principles and Actions*; Lancaster, J., Jr., Ed.; Academic Press: New York, 1996.

(13) Kim, C. H.; Hollocher, T. C. *J. Biol. Chem.* **1984**, *259*, 2092−2099.

(14) (a) Macartney, D. H. *Rev. Inorg. Chem.* **1988**, *9*, 101−151. (b) Baraldo, L. M.; Forlano, P.; Parise, A. R.; Slep, L. D.; Olabe, J. A. *Coord. Chem. Rev.* **2001**, *219*−*221*, 881−921.

(15) Carducci, M. D.; Pressprich, M. R.; Coppens, P. *J. Am. Chem. Soc.* **1997**, *119*, 2669−2678.

(16) Fomitchev, D. V.; Bagley, K. A.; Coppens, P. *J. Am. Chem. Soc.* **2000**, *122*, 532−533.

(17) Coppens, P.; Novozhilova, I.; Kovalevsky, A. *Chem. Rev.* **2002**, *102*, 861−884.

(18) Frisch, M. J.; Trucks, G. W.; Schlegel, H. B.; Scuseria, G. E.; Robb, M. A.; Cheeseman, J. R.; Zakrzewski, V. G.; Montgomery, J. A.; Stratman, R. E.; Burant, J. C.; Dapprich S.; Millam, J. M.; Daniels, A. D.; Kudin, K. N.; Strain, M. C.; Farkas, O.; Tomasi, J.; Barone, V.; Cossi, M.; Cammi, R.; Mennucci, B.; Pomelli, C.; Adamo, C.; Clifford, S.; Ochterski, J.; Petersson, G. A.; Ayala, P. Y.; Cui, Q.; Morokuma, K.; Malick, D. K.; Rabuck, A. D.; Raghavachari, K.; Foresman, J. B.; Cioslowski, J.; Ortiz, J. V.; Baboul, A. G.; Stefanov, B. B.; Liu, C.; Liashenko, A.; Piskorz, P.; Komaromi, I.; Gomperts, R.; Martin, R. L.; Fox, D. J.; Keith, T.; Al-Laham, M. A.; Peng, C. Y.; Nanayakkara, A.; Gonzalez, C.; Challacombe, M.; Gill, P. M. W.; Johnson, B. G.; Chen, W.; Wong, M. W.; Andres, J. L.; Gonzales, C.; Head-Gordon, M.; Replogle, E. S.; Pople, J. A. *Gaussian 98*; Gaussian: Pittsburgh, PA, 1998.

(19) Becke, A. D. *J. Chem. Phys.* **1993**, *98*, 5648−5652.

(20) Lee, C.; Yang, W.; Parr, R. G. *Phys. Rev.* **1988**, *B37*, 785−789.

(21) Casida, M. E.; Jamorski, C.; Casida, K. C.; Salahub, D. R. *J. Chem. Phys.* **1998**, *108*, 4439−4449.

(22) Stratmann, R. E.; Scuseria, G. E.; Frisch, M. J. *J. Chem. Phys.* **1998**, *109*, 8218−8224.

(23) Foresman, J. B.; Keith, T. A.; Wiberg, K. B.; Snoonian, J.; Frisch, M. J. *J. Phys. Chem.* **1996**, *100*, 16098−16104.

Results and Discussion

General Mechanism. The mechanism of reactions 1−4 has been considered on the basis of a common pattern for different B nucleophiles.[4−9]

$$[Fe(CN)_5NO]^{2-} + B^n \rightleftarrows \{Fe(CN)_5NO{\cdot}B\}^{n-2} \quad (5)$$

$$\{Fe(CN)_5NO{\cdot}B\}^{n-2} + OH^- \rightleftarrows [Fe(CN)_5H_2O]^{n-3} + \text{products} \quad (6)$$

Equations 5 and 6 are supported by trustable evidence for the overall stoichiometries and the general way the reaction rates increase with the concentration of OH^-. Evidence on the reversibility of eqs 5 and 6 is conclusive for the cases when $B = OH^-$, reacting with either NP or other $\{MX_5NO\}$ complexes[6] and has also been found for the reactions of hydrazine and phenylhydrazine with $[RuCl(NO)(das)_2]^{2+}$ [das = *o*-phenylenebis(dimethylarsine)].[25] In the reactions of NP with $B = SH^-$, SR^-, and SO_3^{2-},[26−28] the intense red colors and the IR spectra suggest that the adducts decay after formation. The structures of the intermediates have not been clearly elucidated in most cases, though a crystal structure has been obtained for *cis*-$[RuCl(bpy)_2\{N(O)SO_3\}]$.[29]

Experimental results and mechanistic analysis led to the following values for the forward nucleophilic rate constants in eq 5, associated with reactions 1−4: k_5 (M^{-1} s^{-1}) = 0.43 (hydrazine, 25 °C, I = 0.1 M),[7] 4.6 (hydroxylamine, at pH 9, 26 °C, I = l M),[8] and 0.2 (azide, 23 °C, I = 1 M).[8] Ammonia is a poor nucleophile toward NP in aqueous alkaline solutions.[9] An estimation of the nucleophilic rate constant of ca. 10^{-4}−10^{-5} M^{-1} s^{-1} (50 °C)[9b] showed it to be much lower than the one for OH^-, k = 0.55 M^{-1} s^{-1} (25 °C, I = 1 M).[6] Significantly higher values of k_5 have been measured for the more polarizable sulfur binding nucleophiles, ca. 10^2−10^4 M^{-1} s^{-1}.[26,27] The differences in the values of k_5 still allow to include most of the studied electrophilic reactions of nitrosyl under a common mechanistic framework, as described by eqs 5 and 6.

DFT Calculations for Adduct Formation Reactions (Eq 5). As detailed before, direct spectral evidence on the transient adducts is generally scarce. No intermediate spectral traces could be found in the reactions of hydrazine or NH_3 with NP (eqs 1 and 3).[7,9] When available, as for the case of the reactions of NP with hydroxylamine and azide (eqs 2 and 4), it becomes difficult to extract conclusive evidence about their structure from the analysis of the spectroscopic data.[8,30] This fact makes increasingly valuable the information that can be derived from theoretical calculations. Therefore, reactions 2−4 have been analyzed by means of the application of DFT theory, following the same procedure previously applied to study reaction 1.[7] The results for hydrazine are included for the sake of comparison.

Several consecutive steps were considered in the reaction profiles for eqs 1−4, associated with the existence of stable intermediates that result from the theoretical calculations. *The theoretical identification* of stable intermediates has been based in geometry optimization procedures, which afforded evidence for the existence of true minima in the potential hypersurfaces. The first step is defined by the stabilization of a NP-nucleophile adduct (first entries in Figures 1−3), which further deprotonates to give a second stable intermediate. The structures of both adducts are very similar, and similar also for the different nucleophiles, in the characteristics of the Fe−N(O)N moiety. While the first step, associated with the formation of the protonated adducts, is uphill in energy at about 15 kcal/mol, the species are stabilized by deprotonation at 31 kcal/mol. Table 1 summarizes the relevant calculated distances, angles, and IR frequencies. Intense bands are calculated for these second adducts around 410 nm, associated with metal-to-ligand charge-transfer (MLCT) transitions centered in the NO moieties.

In the adducts, the FeNO and FeNN angles are close to 125 and 130°, respectively, whereas the Fe−N and N−O bond distances are significantly elongated relative to the ones in NP, revealing a strong decrease in the bond order. The $N-N_1$ and $N_1-N_2(O)$ distances agree with those found in the literature for the corresponding complexes.[31,32] The Fe−C and C−N distances do not change significantly upon adduct formation, showing that reactivity is mainly associated with changes in the {MNO} fragments. Computed values for the relevant IR frequencies agree with expectations: the values of $\nu_{NOH(N)}$ and $\nu_{NNH(N)}$ are in the region of stretching and rocking vibrations found for hydrazine and other complexes, and the ν_{CN} values are those expected for Fe(II) pentacyano complexes containing π-acceptor L ligands.[14,33]

The above results indicate that a linear to bent transformation of the FeNO moiety occurs upon formation of the different adducts. This was also observed for the OH^--addition reactions to different $\{MX_5NO\}$ complexes.[6] Bending can be anticipated considering that the addition process involves a two-electron transfer to the antibonding LUMO, highly delocalized in the FeNO moiety, with mainly π^*_{NO}

(24) (a) Gorelsky, S. I.; Lever, A. B. P. *Int. J. Quantum Chem.* **2000**, *80*, 636−645. (b) Delley, B.; Schefer, J.; Woike, Th. *J. Chem. Phys*. **1997**, *107*, 10067−10074. (c) Boulet, P.; Buchs, M.; Chermette, H.; Daul, C.; Gilardoni, F.; Rogemond, F.; Schlapfer, C. W.; Weber, J. *J. Phys. Chem. A* **2001**, *105*, 8991−8998.

(25) (a) Douglas, P. G.; Feltham, R. D.; Metzger, H. G. *J. Am. Chem. Soc.* **1971**, *93*, 84−90. (b) Bottomley, F.; Kiremire, E. M. R. *J. Chem. Soc., Dalton Trans.* **1977**, 1125−1131.

(26) Rock, P. A.; Swinehart, J. H. *Inorg. Chem*. **1966**, *5*, 1078−1079.

(27) (a) Johnson, M. D.; Wilkins, R. G. *Inorg. Chem*. **1984**, *23*, 231−235. (b) Schwane, J. D.; Ashby, M. T. *J. Am. Chem. Soc*. **2002**, *124*, 6822−6823.

(28) Andrade, C.; Swinehart, J. H. *Inorg. Chem*. **1972**, *11*, 648−650.

(29) Bottomley, F.; Brooks, W. V. F.; Paez, D. E.; White, P. S.; Mukaida, M. *J. Chem. Soc., Dalton Trans.* **1983**, 2465−2472.

(30) In the reactions of NP with azide and hydroxylamine, the absorbance changes at 510 and 440 nm, respectively, are probably not related to the evolution of the adduct intermediates. Fast coordination of excess nucleophile into the aqua ion and further reactions (aquation of the azide or hydroxylamine complexes or disproportionation of the hydroxylamine-bound product) are possible complicating features. Nevertheless, the measured rate constants in both cases seem to reflect the slow adduct-formation processes, through the measurement of products arising in fast reactions occurring afterward (cf. ref 8).

(31) Heaton, B. T.; Jacob, C.; Page, P. *Coord. Chem. Rev*. **1996**, *154*, 193−229.

(32) Wieghardt, K. *Adv. Inorg. Bioinorg. Mech.* **1984**, *2*, 213−274.

(33) Nakamoto, K. *Infrared and Raman Spectra of Inorganic and Coordination Compounds*, 4th ed.; Wiley: New York, 1986.

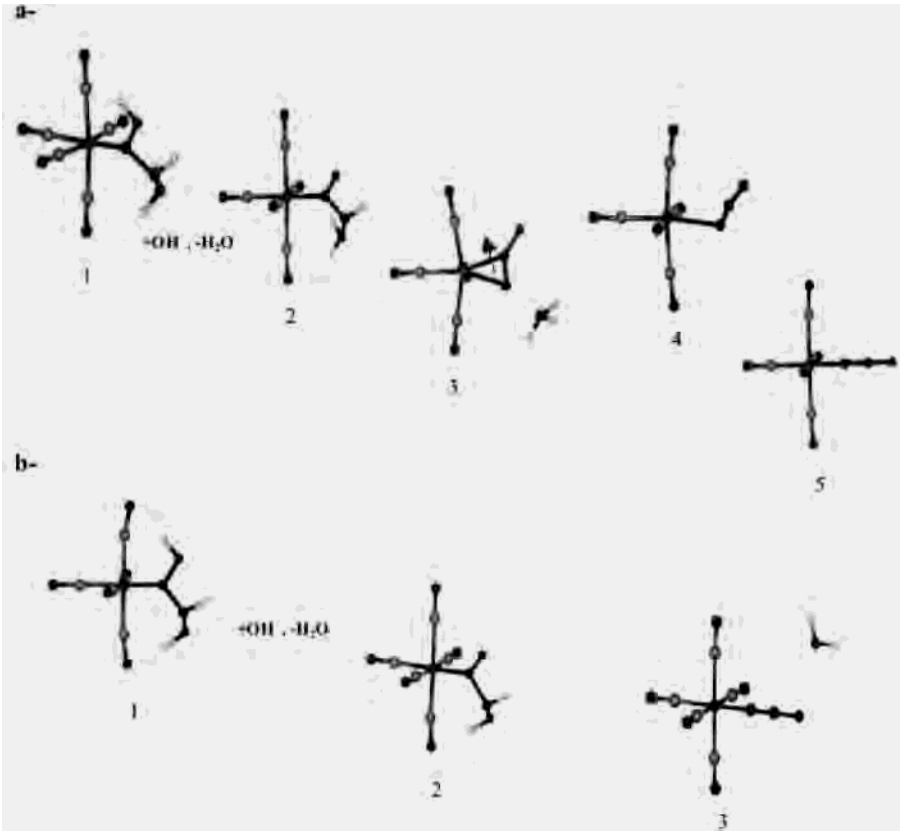

Figure 1. (a) Schematic representation of the initial steps involved in the reaction of $[Fe(CN)_5NO]^{2-}$ with hydrazine, rendering the N_2O-bound intermediates. The structures correspond to singular points in the potential hypersurface, calculated at a B3LYP/6-31G** level. Relative energies (*y* coordinate) are not drawn at scale. Arrows indicate changes in the molecule that lead to the next step. Key (from left to right): 1, $[(NC)_5FeN(OH)NHNH_2]^{2-}$; 2, $[(NC)_5FeN(O)NHNH_2]^{3-}$; 3, $[(NC)_5Fe(\eta^2\text{-}N_2O)]^{3-}$; 4, TS structure; 5, $[(NC)_5Fe(\eta^1\text{-}N_2O)]^{3-}$. (b) Same for hydroxylamine. Key (from left to right): 1, $[(NC)_5FeN(OH)NHOH]^{2-}$; 2, $[(NC)_5FeN(O)NHOH]^{3-}$; 3, $[(NC)_5Fe(\eta^1\text{-}N_2O)]^{3-}$.

character.[34] The process triggers a change of hybridization at the N atom of nitrosyl, from sp to sp^2.

The addition reactions with OH^- have been described as an energy costly process, the cost associated with the modifications of bonds and angles of the MNO and OH^- reactants upon conversion to the $M-NO_2H$ adducts. This description is supported by DFT calculations and by the experimental trends in the activation enthalpies for the different $\{MX_5NO\}$ complexes.[6] It is likely that similar reorganization changes occur upon adduct formation in reactions 1−4, thus giving support to the interpretation of k_5 values as related to slow processes followed by fast adduct decompositions. This interpretation is also compatible with the failure in obtaining spectral information for the adduct intermediates in reactions 1−4.

A particular situation is found for the azide adduct, for which different structures have been proposed in the literature. The formation of a cyclic addition product has been previously anticipated for the reaction of azide with *trans*-$[RuClNO(das)_2]Cl_2$,[35] while a linear addition mode has been proposed for its reaction with NP.[8] Our DFT calculations do not converge to a stable linear minimum. Instead, they provide structural and spectroscopic information supporting the stability of the cyclic azide−NP adduct.

Adduct Decomposition Processes. Figures 1−3 display the results for the conversion of the adduct intermediates into new stable species preceding the production of the $[Fe(CN)_5H_2O]^{3-}$ ion and the release of gaseous products. The DFT calculations are capable of identifying additional energy minima. The species that complete the description of the reaction coordinate for the different reactions are in agreement with what can be established on the basis of the available experimental evidence.

(a) N_2O-Bound Intermediates for B = N_2H_4 and NH_2OH. For the reactions of nitrosyl complexes with hydrazine, the stoichiometry described by eq 1 represents a novel situation.[7] The formation and release of N_2O and NH_3 is quite unusual, because N_2 is the common product of hydrazine oxidations.[36] Early work with $[MCl(das)_2NO]^{2+}$ (M = Ru, Os) has shown bound azide as the product of nucleophilic addition, for which a nitrosohydrazine adduct intermediate has been proposed.[25] A similar mechanism was suggested for $[Ru(NH_3)_5NO]^{3+}$. In this case, the azide product was proposed to evolve to a mixture of N_2-bound and N_2O-bound pentaammine complexes at −23 °C.[37] The alternative mechanisms responsible for the different products found in the hydrazine addition reactions with different $\{MX_5NO\}$

(34) Westcott, B. L.; Enemark, J. H., in *Inorganic Electronic Structure and Spectroscopy, Volume II: Applications and Case Studies*; Solomon, E. I., Lever, A. B. P., Eds.; Wiley: New York, 1999; pp 403−450.
(35) Douglas, P. G.; Feltham, R. D. *J. Am. Chem. Soc.* **1972**, *94*, 5254−5258.
(36) Stanbury, D. M. *Prog. Inorg. Chem.* **1998**, *47*, 511−561.
(37) Bottomley, F.; Crawford, J. R. *J. Am. Chem. Soc.* **1972**, *94*, 9092−9095.

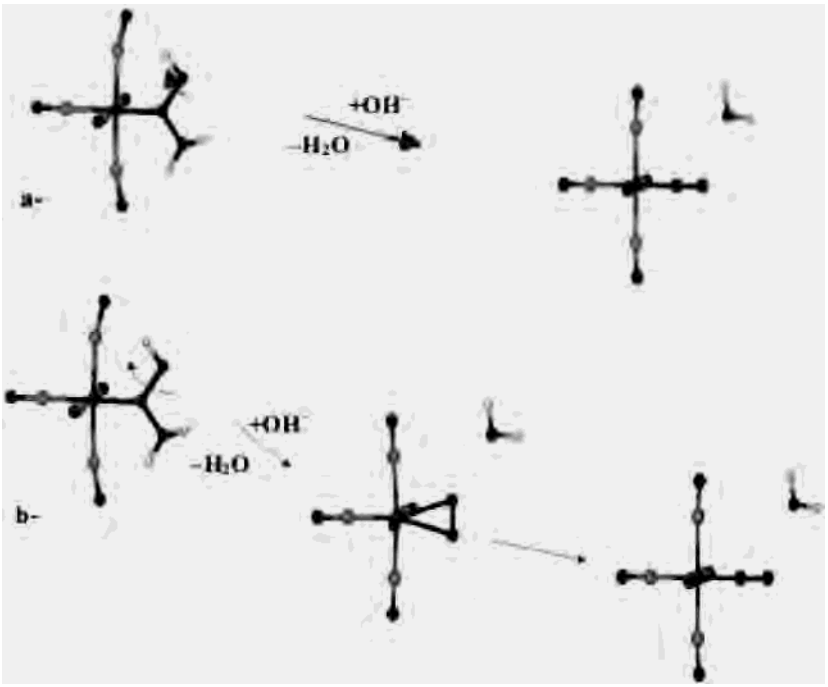

Figure 2. Structures involved in the decomposition of the adduct intermediate resulting from the reaction of [Fe(CN)$_5$NO]$^{2-}$ with NH_3. (a) Only the formation of the linear, η^1-N_2 complex is considered. (b) The formation of η^2-N_2 as an intermediate step is also included. The structures correspond to singular points in the potential hypersurface, calculated at a B3LYP/6-31G** level. Relative energies are not drawn at scale. Arrows indicate changes in the molecule that lead to the next step.

fragments, as well as with HNO_2,[38] have been recently discussed.[7] On the other hand, the addition of NH_2OH into [IrX$_5$NO]$^-$ (X = Cl$^-$, Br$^-$)[39] and [Ru(NH$_3$)$_5$NO]$^{3+}$ shows the same stoichiometry as eq 2. For the latter compound, the proposed adduct, [Ru(NH$_3$)$_5$N(O)NHOH]$^{2+}$, led to the [Ru(NH$_3$)$_5$N$_2$O]$^{2+}$ ion, which has been isolated as a dihalyde salt.[37]

In Figure 1a, for B = N_2H_4, the first minimum after NH_3 release corresponds to η^2-N_2O, which is 43 kcal/mol more stable than the deprotonated adduct coordination mode.[7] For the [Ru(NH$_3$)$_5$N$_2$O]$^{2+}$ ion,[37,40a] it has been assumed that N_2O binds in a η^1 linear mode through the terminal N atom,[40b] giving a structure supported by theoretical calculations.[40c] The η^1 linear mode, shown in Figure 1a, (6 kcal/mol more stable than the previous one) defines the fourth minimum in the potential hypersurface, according to our calculations. The reaction sequence that we predict justifies η^1 and η^2 coordination modes, defining stable intermediate structures in the reaction coordinate. However, the linear η^1 coordination is not easily attained in a single step from the initial adduct, as it is the η^2 one, which only needs angular reorganization after NH_3 releasing. The transition-state (TS) structure calculated for the conversion of η^2-N_2O into η^1-N_2O (fourth entry, Figure 1a) stands 7 kcal/mol higher in energy than the η^2 state. Although never proposed before, the existence of the [Fe(CN)$_5$N$_2$O]$^{3-}$ η^1 and η^2 complexes is quite understandable, given the similarities in the chemistry of pentaammino and pentacyano complexes and the existence of η^1 and η^2-N_2 complexes, related to the first ones. The pentacyano complexes are more labile, however, precluding the isolation of N_2O complexes as stable solid salts.[41]

Figure 1b shows the structures that result from a similar calculation, associated this time with the hydroxylamine adduct decomposition. It can be seen that the evolution of the first adduct *only* allows the stabilization of the η^1-N_2O intermediate, which is formed in a single process, with an energy decrease of 27 kcal/mol.

It is a remarkable fact that the mechanisms of adduct decompositions differ significantly for the hydrazine and hydroxylamine complexes. In the hydrazine adduct, the oxygen atom of the resulting N_2O is obviously the one previously existing in NP. With hydroxylamine, however, the labeling experiments have demonstrated that the O atom in N_2O comes from this reactant.[8] The NO-belonging O atom is released as water, leaving the linear intermediate, after angular reorganization, in a single step. The main structures involved, shown in Figure 1b, are true minima in the potential hypersurface. In this case, the proposed mechanism is substantially supported by the experimental evidence. The different kinetic stabilization of the intermediates offers an explanation to this crucial mechanistic feature that differentiates nucleophiles that are structurally as similar as hydrazine and hydroxylamine.

Table 2 displays the calculated distances, angles, and IR frequencies for both N_2O linkage isomers. The N−N and N−O distances in η^1-N_2O are slightly longer than in free N_2O, but the difference is greater, ca. 0.06 Å, for η^2-N_2O.

(38) Perrott, J. R.; Stedman, G.; Uysal, N. *J. Chem. Soc., Dalton Trans*. **1976**, 2058−2064.
(39) Bottomley, F.; Clarkson, S. G.; Tong, S. B. *J. Chem. Soc., Dalton Trans*. **1974**, 2344−2346.
(40) (a) Armor, J. N.; Taube, H. *J. Am. Chem. Soc*. **1969**, *91*, 6874−6876. (b) Bottomley, F.; Brooks, W. V. F. *Inorg. Chem*. **1977**, *16*, 501−502. (c) Tuan, D. F.; Hoffmann, R. *Inorg. Chem*. **1985**, *24*, 871−876.
(41) (a) Ford, P. C. *Coord. Chem. Rev*. **1970**, *5*, 75−99. (b) Taube, H. *Pure Appl. Chem*. **1979**, *51*, 901−912.

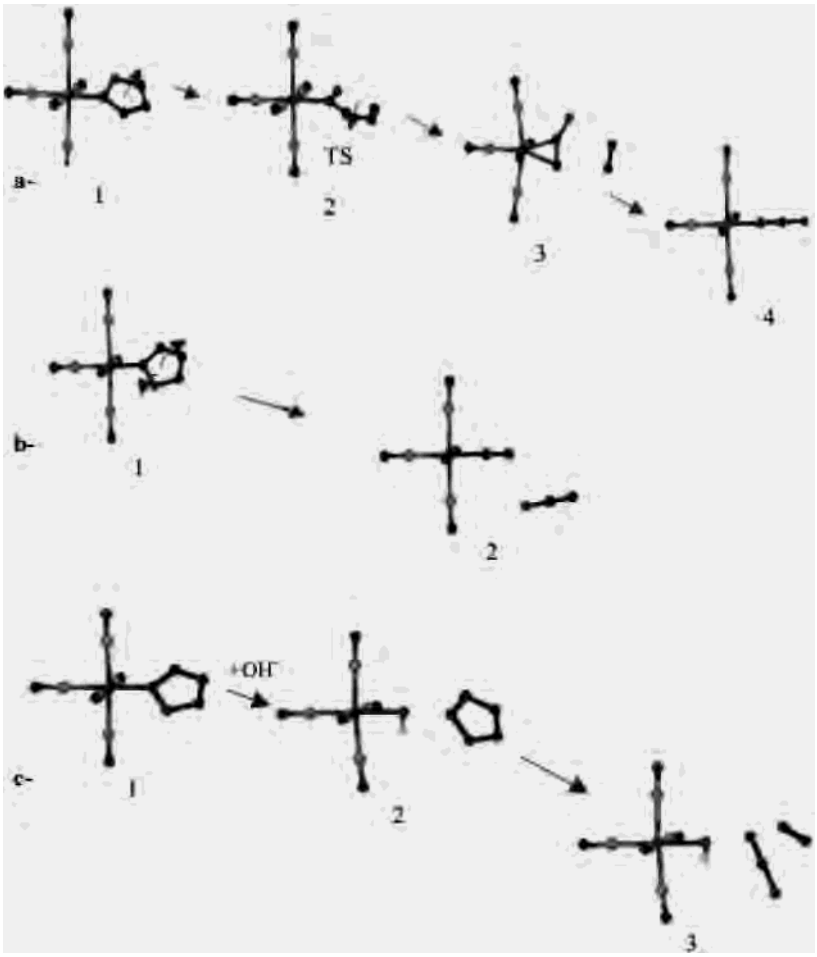

Figure 3. Possible decomposition paths of the cyclic adduct formed by reaction of $[Fe(CN)_5NO]^{2-}$ with azide: (a) N_2 release and stabilization of the N_2O-bound intermediates; (b) N_2O release and stabilization of the N_2-bound intermediate; (c) N_4O release promoted by OH^- substitution. The cyclic species decomposes to give N_2O and N_2 in a reaction that is exothermic at 60 kcal mol^{-1}. The structures correspond to singular points in the potential hypersurface, calculated at a B3LYP/6-31G** level. Relative energies are not drawn at scale. Arrows indicate changes in the molecule that lead to the next step.

Table 1. Calculated Distances (Å), Angles (deg), and Selected IR Frequencies (cm^{-1}) for the Reactant, $[Fe(CN)_5NO]^{2-}$ (NP), and the Deprotonated Adduct Intermediates, $\{Fe(CN)_5NO{\cdot}B\}^{n-2}$, Formed by Reaction with Nucleophile B^n, for $B^n = N_2H_4$, NH_2OH, NH_3, and N_3^-

	FeNO (NP)	FeNO−N_2H_4	FeNO−NH_2OH	FeNO−NH_3	FeNO−N_3^-
Fe−N	1.615	1.785	1.787	1.789	1.825
N−O	1.160	1.376	1.377	1.367	1.443
$N-N_1$[a]		1.365	1.385	1.354	1.310
N_1-N_2[b,c]		1.405	1.403		1.342
F−C, cis	1.959	1.962	1.955	1.960	1.983
Fe−C, trans	1.965	1.972	1.958	1.960	1.971
C−N, cis	1.169	1.172	1.175	1.173	1.175
C−N, trans	1.168	1.172	1.170	1.169	1.175
∠FeNO	179.9	123.0	124.8	125.6	121.3
$\angle FeNN_1$		133.0	130.8	129.0	133.9
$\angle NN_1N_2$[c]		115.8	114.5		109.7
ν_{NOH}[d]		1008, 1041	1006, 1487	989	906
ν_{NNH}[d]		1021, 1160, 1310	751, 1414	819, 1188	1090
ν_{CN}	2160	2127−2172	2125−2176	2122−2172	2130−2143

[a] N_1: N atom binding to nitrosyl. [b] N_2: N atom binding to N_1. [c] N_2 is O for the case of NH_2OH. [d] H must be replaced by N for the cyclic azide

This seems reasonable on the basis of predictable $\sigma-\pi$ interactions weakening the two bonds. The existence of the η^2 side-bound N_2O intermediate should be considered in the context of the modern developments on the structure of the photogenerated linkage isomers of NO, namely the MS1 and MS2 states (end-on, O-bound "isonitrosyl" ligand and η^2, side-bound, respectively).[15] Interestingly, the FeNN angle of 69.19° is similar to the one found for FeNO in the side on MS2 state of NP, 65.1°. As in the latter MS2, Figure 1a shows that the equatorial ligands are repelled by the side-on N_2O group. The calculated IR results also show significant shifts in the relevant frequencies, consistent with the described geometry changes. Thus, η^1-N_2O shows calculated stretching frequencies for the NNO fragment at 2287 and 1120 cm^{-1}, close to those observed for $[Ru(NH_3)_5NNO]^{2+}$.[40b] In contrast, for η^2-N_2O the calculations render absorption bands at 1812 and 1159 cm^{-1}. The first one, strongly downshifted with respect to the one in the η^1 isomer,

Table 2. Calculated Distances (Å), Angles (deg), and Relevant IR Frequencies (cm^{-1}) for the Stable Intermediates Formed with N_2O and N_2 Ligands after the Decomposition of the Different Adducts Described in the Text

	η^2-N_2O[a,b]	η^1-N_2O[a,b]	η^2-N_2[c,d]	η^1-N_2[c,d]
Fe−N	2.075, 1.992	1.820	2.226, 2.226	1.793
N−O	1.254	1.242		
N−N	1.191	1.138	1.133	1.128
Fe−C, cis	1.975	1.990	1.988	1.989
Fe−C, trans	1.949	1.962	1.928	1.976
C−N, cis	1.175	1.176	1.177	1.176
C−N, trans	1.175	1.176	1.177	1.176
∠FeNO	142.5			
∠FeNN	76.8	179.8	75.3	180.0
∠NNO	140.6	179.8		
ν_{NNO}	1159, 659	2287, 1120		
ν_{NN}	1812		2100	2167
ν_{CN}	2127−2147	2114−2131	2106−2116	2115−2126

[a] Distances in free N_2O: N−N, 1.1282 Å; N−O, 1.1842 Å.[10] [b] Fundamental IR wavenumbers in free N_2O: ν_1 (asymmetric stretch), 1285 cm^{-1}; ν_2 (bending), 589 cm^{-1}; ν_3 (symmetric stretch), 2224 cm^{-1}.[10] [c] N−N distance in free N_2, 1.10 Å; N−N distance in $[Ru(NH_3)_5(\eta^1\text{-}N_2)]^{2+}$, 1.12 Å.[42] [d] See text for comparisons with η^1- and η^2-complexes of $[Os(NH_3)_5N_2]^{2+}$.[16]

probably reflects the strong π-interactions of iron with the side-on N═N moiety. The cyanide-stretching values can be interpreted in terms of the competing π-acid abilities of cyanide vs the N_2O ligands.

In relation to the UV−vis spectra, calculated MLCT bands appear at 323 nm for the η^2-N_2O intermediate (with a shoulder at 451 nm) and at 265 nm for the η^1-N_2O one. They correspond, in both cases, to transitions from an orbital centered in the metal to the LUMO, delocalized in the N_2O ligand. The 265 nm band is consistent with the one found at 233 nm for the linear $[Ru(NH_3)_5N_2O]^{2+}$ ion.[40b]

(b) N_2-Bound Intermediates for B = NH_3. The stoichiometry of the reaction of NP with NH_3 (eq 3) has been early studied.[9] This reaction is very important for the chemistry of pentacyano-L-ferrates, because it allows the isolation of salts of the $[Fe(CN)_5NH_3]^{3-}$ ion,[9c] a suitable precursor for the synthesis of complexes with different L ligands.[14] A similar stoichiometry has been only found for the addition of NH_3 into the $[IrX_5NO]^-$ ions (X = Cl^-, Br^-).[39]

The maximum N_2 yield for reaction 3 was obtained at pH 10 (1 M NH_4Cl). Whereas higher pH's favor OH^- attack, lower pH's favor protonation of ammonia. Nucleophilic addition of NH_3 is precluded in both cases.[9b] Figure 2a shows the structure of the calculated adduct intermediate and of the η^1-N_2 isomer that is attained by its further conversion. The system is stabilized in 20 kcal/mol in this reaction, according to the calculations. The end-on linear coordination mode is well-known to be a stable form for dinitrogen bound to transition metal centers.[42] The formation of this Fe−N_2 intermediate appears as reasonably predictable, following a three-electron transfer to NP with further proton and OH^- loss. The calculated geometrical and IR parameters are displayed in Table 2.

The presence of η^2-N_2 in irradiated samples of $[Os(NH_3)_5(\eta^1\text{-}N_2)][PF_6]_2$ has been recently reported and supported by experimental and theoretical evidence.[16] We found stable energy minima for both the η^1-N_2 and the η^2-N_2 intermediates bound to $[Fe(CN)_5]^{3-}$. We calculate the η^1-N_2 isomer more stable by 23 kcal/mol than the η^2-N_2 one. For the reaction shown in Figure 2b, the adduct's energy is lower than that of η^2-N_2, and therefore, we do not expect this intermediate to occur. Table 2 displays the relevant structural and spectroscopic parameters. In the same way previously described for N_2O, it becomes evident that η^2-N_2 has a significantly elongated Fe−N distance compared to the one in η^1-N_2. These elongated Fe−N distances, as well as the FeNN angle, 75.23°, are very close to those observed in $[Os(NH_3)_5(\eta^2\text{-}N_2)]^{2+}$. The N−N distances in both isomers approach 1.13 Å, a value close to the one in $[Ru(NH_3)_5N_2]^{2+}$, 1.12 Å, and expectedly longer than in free N_2 molecule, 1.098 Å.[43,44] The stretching N−N frequencies for the pentacyanoferrate N_2 complexes were 2167 and 2100 cm^{-1} for the η^1 and η^2 isomers, respectively. The latter shows a lower value, which is predictable on the basis of the consideration of the strong π-interactions responsible of weakening the N−N bond. The magnitude of the shift is however smaller than in $[Os(NH_3)_5N_2]^{2+}$: 2025 and 1838 cm^{-1} for the stretchings in η^1 and η^2, respectively, due to the stronger interactions that imply bonding to an osmium center.

Reaction 3 could be envisaged as a basis for the catalytic reduction of nitrite to N_2 in the presence of excess ammonia. A $NO_2^- \rightarrow N_2O$ catalytic conversion has been also described for reaction 1.[7] However, the poor rate of NH_3 addition to NP (see above) seriously compromises the possible practical applications of this reaction.[9b]

(c) N_2- and N_2O-Bound Intermediates for B = N_3^-. The reactions of azide with nitrosyl complexes have been largely used for synthetic purposes, with the aim of replacing the nitrosyl ligand by other L's.[2,4] Several $\{MX_5NO\}$ complexes have been found to react according to the stoichiometry shown in eq 4 (MX_5: *trans*-$[RuCl(das)_2]^+$;[35] *trans*-$[RuCl(py)_4]^+$;[45] *cis*-$[Ru(bpy)_2Cl]^+$;[46] $[IrX_5]^{2-}$ (X = Cl^-, Br^-);[39] $[Os(bpy)(Cl)_3]^-$.[47]

Figure 3 shows the calculated decomposition paths for the cyclic adduct, with different possible intermediates. Either the release of N_2 leaving a η^2-N_2O complex which further evolves to the η^1 isomer (Figure 3a) or the competitive release of N_2O leaving a η^1-N_2 complex is probable (Figure 3b). Interestingly, evidence for both reaction paths have been

(42) Hidai, M.; Mizobe, Y. In *Reactions of Coordinated Ligands*; Braterman, P. S., Ed.; Plenum Publ. Corp.: New York, 1989; Vol. 2, pp 53−114.

(43) Leigh, G. J. *Sci. Prog. (Northwood, U.K.)* **1989**, *73*, 389−412.

(44) A side-on dinitrogen nickel complex, $[[(LiPh)_3(Et_2O)_{1-1.5}Ni]_2N_2]_2$, has been reported (cf. ref 41), with a remarkably lengthy N−N distance, 1.35 Å. The dinitrogen ligand binds to both Ni and Li metals and leads to NH_3 in aqueous medium.

(45) (a) Bottomley, F.; Mukaida, M. *J. Chem. Soc., Dalton Trans.* **1982**, 1933−1937. (b) Coe, B. J.; Meyer, T. J.; White, P. S. *Inorg. Chem.* **1995**, *14*, 593−602.

(46) (a) Miller, F. J.; Meyer, T. J. *J. Am. Chem. Soc.* **1971**, *93*, 1294. (b) Adeyemi, S. A.; Miller, F. J.; Meyer, T. J. *Inorg. Chem.* **1972**, *11*, 994−999.

(47) Huynh, M. H. V.; Baker, R. T.; Jameson, D. L.; Laboriau, A.; Meyer, T. J. *J. Am. Chem. Soc.* **2002**, *124*, 4580−4582. The *mer*-$[Os(bpy)(Cl)_3(N(OH)N_3)]$ complex, formulated as an Os^{IV}−azido hydroxoamido species, led to the $[Os^{II}(bpy)(Cl)_3(N_2O)]^-$ complex upon deprotonation, internal electron transfer, and N_2 release. The N_2O complex was isolated as a PPN salt; IR evidence suggests an η^1-coordination mode for N_2O, similar to $[Ru(NH_3)_5N_2O]^{2+}$.[40]

found for $[RuCl(das)_2NO]^{2+}$.[35] On the basis of isotopic substitution experiments starting from $Ru^{15}NO$ and unlabeled azide, equal amounts of $^{14}N^{15}NO$ and $^{14}N^{14}NO$ were found. It was concluded that the cyclic adduct could decompose following both ways, a reaction that would most probably occur after dissociative cleavage of the N_4O species from the metal center. In contrast, the reaction of $FeN^{18}O$ (in NP) with labeled azide $^{15}N^{14}N^{14}N^-$ led only to $^{15}N^{14}N^{18}O$. The authors suggested that either a linear addition mode or a cyclic intermediate exclusively breaking as in Figure 3a could be possible. However, they discarded the latter mode without further foundation.[8]

Our calculations do not lead to a stable energy minimum for the linear addition mode. Moreover, only 10 kcal/mol favors the decomposition mode described in Figure 3b over the one shown in Figure 3a. This calculated figure indicates that the trend could be certainly reversed if different effects, as a simulated environment taking into account the specific cyanide−solvent interactions, are included in the theoretical models. For the decomposition mode of Figure 3a, a TS has been calculated (same figure), which is 18 kcal/mol more stable than the initial adduct, indicative of a nonactivated process. It is characterized by an O−N distance of 2.01 Å and a ONN angle that has slightly increased from 105° (in the adduct) to 120.9° in the TS. The N−N bond that should break in the next step of the reaction has been already elongated to 1.54 Å, compared to the N−N distance of 1.17 Å in N_2. The mechanism depicted in Figure 3b implies an energy decrease close to 60 kcal/mol, measured from the adduct to the final product. Within this scheme, the η^2-N_2 intermediate might appear as an additional step. However, on the basis of the different Fe−N distances for consecutive N atoms in the adduct (1.82, 2.89 Å), we do not consider this 3-step reaction as a predictable path.

A third possibility has to be considered (Figure 3c) for the azide-adduct decomposition mechanism. This implies the initial cleavage of the Fe−N bond, releasing a neutral N_4O cyclic molecule, whose further decomposition results in equal amounts of N_2 and N_2O. The release of N_4O can occur in alkaline media, assisted by OH^- substitution, according to eq 7, with an energy decrease of 10 kcal/mol.

An additional energy decrease of 62 kcal/mol is attained by N_4O decomposition, defining a reaction path which competes with the ones previously described.

$$Fe(CN)_5N_4O]^{3-} + OH^- \rightarrow [Fe(CN)_5OH]^{4-} + N_4O \quad (7)$$

This mechanism is exothermic, attaining an energy release close to 75 kcal/mol/N_2 molecule. Then, although the N_4O molecule cannot be classified like a high energy density material itself[48,49] (HEDM) due to its inherent lability, it can be stabilized through metal coordination, this time implying the Fe atom of the pentacyanoferrate complex. This stabilization may allow the occurrence of a two step process: an initial high energy release of N_4O, followed by a low-energy barrier dissociation ending in N_2 and N_2O. The kinetic study of the first step of this mechanism becomes, thence, a subject of interest in relation to HEDM research.

The potential stabilization of small N_2-related structures through coordination to metal centers has been recently discussed[50] for the case of coordination to Al centers. In this framework, metal catalysis appears as a promising strategy to be considered in the synthesis of HEDM.

Conclusions

DFT calculations have been performed for the reactions of different nitrogen hydrides with NP. The reaction profiles show energy minima indicative of the stabilization of adduct intermediates in the first step of the reactions, attained through additions of the hydrides to the N atom of nitrosyl. The adduct structures reveal that a linear to bent conversion has occurred, associated with a charge transfer from the nucleophile to the FeNO fragment. This results in a population of the antibonding LUMO orbital of the adduct, largely delocalized on this fragment The calculated distances, angles, and IR frequencies for the corresponding adducts agree with the above picture.

The results provide a conclusive structural interpretation for the available kinetic and mechanistic information associated with these reactions. On the basis of the well-defined stoichiometries for the different reactions, which lead to N_2, N_2O, or to equimolar mixtures of them, the DFT calculations also predict the stabilization of linkage isomers of N_2O and N_2 bound to the iron center. The η^2-N_2O isomer is formed as an initial stage of adduct decomposition in the reactions with hydrazine and azide, followed by a conversion to the more stable η^1-N_2O isomer and further release of N_2O to the medium. Interestingly, only the η^1-N_2O isomer is predicted for the reaction of NP with hydroxylamine, revealing the importance of kinetically controlled processes for N_2O formation. Both η^1-N_2 and η^2-N_2 isomers are also predicted as stable species, but only the first one seems to be energetically allowed in the actual reactions of NP with NH_3 and azide. The structural and spectroscopic data calculated for the linkage isomers are entirely consistent with recent experimental X-ray and spectroscopic measurements on related NO and N_2 analogues.

We have shown the utility of modern theoretical procedures to predict and/or confirm the reaction profiles of an important reaction type: the nucleophilic attack to bound nitrosyl. This article appears as a significant contribution, given the environmental importance of denitrification processes, helping to understand the mechanisms involved in the formation and release of N_2 or N_2O products.

Acknowledgment. This work was supported by the Universities of Buenos Aires and La Plata, the Argentinian agencies Anpcyt and Conicet, and the VolkswagenStiftung. J.A.O. and G.L.E. are members of the scientific staff of Conicet.

IC0261880

(48) Hammert, A.; Klapotke, T. M.; Noth, H.; Warchhold, M.; Holl, G.; Kaiser, M.; Ticmanis, U. *Inorg. Chem.* **2001**, *40*, 3570−3575.
(49) Strout, D. L. *J. Phys. Chem. A* **2002**, *106*, 816−818.
(50) Lee, E. P. F.; Dyke, J. M.; Claridge, R. P. *J. Phys. Chem. A* **2002**, *106*, 8680−8695 and references therein.